Journal of Colloid and Interface Science 683 (2025) 1078–1086

Contents lists available at ScienceDirect

Journal of Colloid And Interface Science

journal homepage: www.elsevier.com/locate/jcis

Regular Article

Water-membrane partition and the mutant selection window of antimicrobial peptides: insights from liposome studies

Federico Carneri [a,b], Cassandra Troiano [a], Giuseppe Giaquinto [a], Daniela Roversi [a], Henrik Franzyk [c], Lorenzo Stella [a,*]

[a] Department of Chemical Science and Technologies, Tor Vergata University of Rome, 00133 Rome, Italy
[b] Photoinduced Processes and Technologies Doctoral School, Department of Chemistry, Biology and Biotechnology, Perugia University, 06123 Perugia, Italy
[c] Department of Drug Design and Pharmacology, University of Copenhagen, DK-2100 Copenhagen, Denmark

HIGHLIGHTS

- Antimicrobial concentrations in the mutant selection window do not kill all bacteria.
- Antimicrobial peptides exert similar heterogeneous effects on a liposome population.
- The apparent heterogeneous response arises from water-membrane partition.
- Vesicle poration actually takes place at a well-defined threshold of bound peptides.
- For the peptides investigated, the threshold depends on peptide size only.

GRAPHICAL ABSTRACT

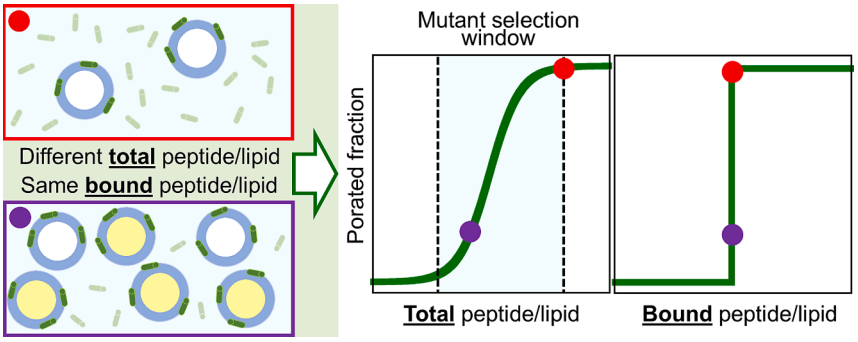

ARTICLE INFO

Keywords:
Peptide-membrane association
Phospholipid membranes
Pore formation
Fluorescence spectroscopy
Mutant selection window

ABSTRACT

The mutant selection window (MSW) is a range of antimicrobial concentrations, where some bacteria are killed, while others survive. Within this interval resistance may develop. Antimicrobial peptides (AMPs) are a promising class of antimicrobials that generally act by perturbing the integrity of bacterial membranes. Their MSW is typically narrower than that of traditional antibiotics, but it still encompasses about one order of magnitude of peptide concentrations. Phenotypic or genetic differences between individual cells may cause this heterogeneous bacterial response to AMPs. Therefore, we minimized the system complexity by investigating pore formation in liposomes with homogeneous size and composition. Surprisingly, the AMPs novicidin, P9-4, and Sub3 formed pores only in a fraction of vesicles, over a wide range of total peptide concentrations. By characterizing the water/membrane partition equilibrium of these three AMPs, we were able to report the vesicle-perturbing activity as a function of the membrane-bound peptide concentration. In this case, the curves became essentially step functions with well-defined (bound) concentration thresholds at which pores were formed in all liposomes. Therefore, the apparent heterogeneous effects of AMPs on vesicles were actually determined by variations in the fraction of membrane-bound peptides under different conditions, due to water-membrane partition. Unexpectedly, the thresholds coincided for all peptides in terms of bound amino acids per lipid (~0.4), suggesting that the mechanism of pore formation primarily depends on the surface coverage by the AMPs.

* Corresponding author at: Department of Chemical Science and Technologies, Tor Vergata University of Rome, Via della ricerca scientifica, 1, 00133 Rome, Italy.
E-mail address: stella@stc.uniroma2.it (L. Stella).

https://doi.org/10.1016/j.jcis.2024.12.099
Received 24 September 2024; Received in revised form 11 November 2024; Accepted 15 December 2024
Available online 19 December 2024

1. Introduction

Antimicrobial resistance (AMR) is a rapidly escalating global issue, where pathogenic bacteria evolve towards declining susceptibility to antibiotics, making infections difficult to treat or even untreatable [1]. Without intervention, it is estimated that global deaths attributable to AMR could reach 10 million annually by 2050 (which is a 10-fold increase from the current situation) [2]. Amidst the AMR crisis, antimicrobial peptides (AMPs) have emerged as promising alternatives to conventional antibiotics [3]. These natural cationic, amphipathic peptides play a crucial role in the innate immunity of multicellular organisms and in bacterial interspecies competition. They target bacterial pathogens through multiple mechanisms, but most importantly by disrupting their membranes by a purely physico-chemical process, due to their amphipathic properties. AMPs are receiving considerable attention for their clinical potential, due to their very limited propensity to induce bacterial resistance [3]. This characteristic is linked to their mechanism of action (which does not target a specific protein and does not require entry into the cytosol), their fast killing kinetics, but also their pharmacodynamic properties [3–4].

Inappropriate dosing of antibiotics is an important cause of AMR [5]. Resistance can evolve when drugs are used at concentrations of intermediate efficacy, where some bacteria are killed, while others survive, thus creating a selection pressure [3]. This antimicrobial concentration range, in which resistant mutants can be selected for, has been termed the “mutant selection window” (MSW) [4,6]. Interestingly, the typical MSWs for AMPs are narrower than those seen for traditional antibiotics, and combinations of different AMPs may further reduce this unsafe concentration range [3–4,7–11]. All the same, even AMPs have MSWs that span several orders of magnitude of concentrations [4,12].

A more complete understanding of the determinants for the MSW is fundamental to enable design of novel antimicrobials with improved properties and to establish the optimal dosing of currently available drugs. Traditionally, partial killing of a bacterial population has been attributed to genetic differences between individual cells. However, heterogeneities in drug activity within a population of genetically identical bacteria have been demonstrated by single cell experiments [13–14]. In principle, this observation might have several possible explanations, including phenotypic cell-to-cell differences (such as different stages in the cell cycle) and variations in the amount of drug accumulating in each cell [13–14]. Fortunately, the distinct physico-chemical mechanism of action of AMPs allows for a significant simplification of the problem, since the membrane-perturbing activity of these molecules may be approximated by assays on artificial vesicles, *e.g.* by following the release of a fluorophore entrapped in the aqueous lumen of liposomes [13,15–16]. Liposomes can be produced with extremely homogeneous size and lipid composition, thus ruling out most possible causes of variability [13,15]. Therefore, it is quite puzzling that AMPs often only perturb a fraction of the vesicle population, causing release of their contents over a wide range of peptide to lipid ratios [17–24] even in single-liposome studies [13]. This range is typically about one order of magnitude when the lipid concentration is fixed, while the peptide concentration is varied [17–20,22–24]. It becomes significantly wider (2–4 orders of magnitude), when the peptide to lipid ratio is varied by changing the lipid concentration (keeping the AMP concentration fixed) [21–22].

The goal of the present study is to understand the origin of the heterogeneous effects of AMPs on a liposome population over a significant range of peptide to lipid ratios. To this end, we selected three model membrane-active antimicrobial peptides (novicidin, P9-4, and Sub3; see Table 1) that are quite different in terms of sequence, charge and activity [25–34] and contain at least one fluorescent amino acid (required for our spectroscopic studies) in their sequences. Their main properties are summarized in Table 1. Novicidin [25–28]and P9-4 [29] are known to be membranolytic, and they were among the peptides previously investigated in our study on the inoculum effect [30]. The mechanism of action of Sub3 involves membrane targeting too, albeit intracellular effects might contribute to bacterial killing by this AMP [34]. We focused on membrane-active peptides in order to ensure that peptide-induced pore formation would occur in vesicle mimics of cell membranes.

2. Materials and methods

2.1. Materials

Lipids were purchased from Avanti Polar Lipids (Alabaster, Al, USA). Spectroscopic grade solvents were obtained from Carlo Erba Reagenti (Milano, Italy). 5(6)-Carboxyfluorescein (CF), Triton-X 100 and Sephadex-G50 were purchased from Sigma Aldrich (St. Louis, MO, USA). Peptides were synthesized on a CEM Liberty™ microwave peptide synthesizer by using microwave-assisted Fmoc-based solid-phase peptide synthesis, as previously reported [35]. An H-Rink-Amide resin from Matrix Innovation (loading 0.50 mmol/g; 0.1 mmol; 100–200 mesh) was used as solid support. Coupling of Nα-Fmoc-protected amino acid building blocks (5.0 equiv for the CEM™ Liberty Blue, with acid-labile tBu/Trt/Boc/Pbf as side-chain protecting groups) in dimethylformamide (DMF) were performed with diisopropylcarbodiimide (DIC, 0.5 M in DMF; 5.0 equiv) and ethyl (hydroxyimino)cyanoacetate (OxymaPure®, 0.5 M in DMF, 5.0 equiv) in a 0.10 mmol scale. Each residue was inserted via double-coupling (each at 75 °C for 10 min). Fmoc deprotection: 20 % (v/v) piperidine in DMF (2 × 3 min at room temp.). Side chain deprotection and cleavage were performed simultaneously with trifluoroacetic acid (TFA), H_2O and triisopropylsilane (95:2.5:2.5; 2 × 30 min, each with 5 mL, while shaking at rt). Filtrates were collected, and the resin was then eluted with CH_2Cl_2 (2 mL). The filtrates were combined and concentrated in vacuo, and then co-evaporated with toluene (2 × 5 mL). Preparative HPLC of crude peptides was performed on a Phenomenex Luna Omega Polar C18 column (250 × 30 mm; particle size: 5 μm; pore size: 100 Å), using a Shimadzu Prominence system. Eluting with H_2O-acetonitrile (MeCN) gradients with 0.1 % trifluoroacetic acid (TFA) added to the eluents (A: 5:95 MeCN–H2O + 0.1 % TFA; B: 95:5 MeCN–H_2O + 0.1 % TFA) with UV detection at λ = 220 nm. The purity of each peptide was determined by analytical HPLC using a Phenomenex Luna C18 Omega Polar column (4.6 × 150 mm; particle size: 3 μm; pore size: 100 Å) using the same eluents as for preparative HPLC in a linear gradient from 0 % to 60 % during 15 min (flow rate: 0.5 mL/min) and UV detection at 220 nm.

Peptide purity and HPLC retention times are reported in Table S1 in the Supporting Information. Further details on peptide characterization are provided in the original references [28–31,33,36].

2.2. Liposome preparation

Large unilamellar vesicles (LUVs) composed of POPE (1-palmitoyl-2-oleoyl-*sn*-glycero-3-phosphatidylethanolamine) and POPG (1-palmitoyl-2-oleoyl-*sn*-glycero-3-phospho-(1′-*rac*-glycerol)) (7:3 M ratio) were prepared by dissolving the lipids in a 1:1 (v/v) $CHCl_3$/MeOH (methanol) solution. The solvent was then evaporated in a rotary vacuum system, until a thin film was formed. Complete evaporation was ensured by applying a rotary vacuum pump for at least 2 h. Then, the lipid film was hydrated with a 10 mM phosphate buffer (pH = 7.4), prepared by using

Table 1
Peptides investigated in the present study.

	Sequence	AA[a]	Q[b]	Q/AA
Novicidin	KNLRRIIRKGIHIIKKYF-NH_2	18	+8	+0.44
P9-4	KWRRWIRWL-NH_2	9	+5	+0.56
Sub3	RRWRIVVIRVRR-NH_2	12	+7	+0.58

[a] Number of residues.
[b] Electrostatic charge (under physiological pH).

ultrapure water and containing 140 mM NaCl and 0.1 mM ethylenediaminetetraacetic acid (EDTA) (buffer A). The liposome suspension was vigorously stirred, and, after 10 freeze and thaw cycles, it was extruded through two stacked polycarbonate membranes with 100 nm pores, for 31 times. In CF leakage experiments, the lipid film was hydrated with a CF solution at a self-quenching concentration (30 mM) [19], titrated to pH 7.4 with NaOH, and containing 10 mM phosphate buffer and 80 mM NaCl to make it isotonic to dilution buffer A (270 mOsm) [37]. Liposomes were separated from the unencapsulated dye by gel filtration on a 40 cm Sephadex G-50 column, and liposomes were kept at room temperature during the time required for the experiments. The final lipid concentration was determined with the Stewart phospholipid assay [38].

2.3. Membrane-perturbing activity experiments

Perturbation of membrane permeability was determined by measuring the release of the CF fluorophore. These experiments were performed on an Infinite M200 Pro (Tecan, Salzburg, Austria) microplate reader. Dye release was measured by the increase in fluorescence intensity caused by the reduction in self-quenching when the CF leaked from the liposomes and was diluted in the outer solution [39]. A black 96-well, flat-bottom polystyrene, nonbinding plate (Model 655900, Greiner bio-one, Germany) was filled first with liposome solutions of different lipid concentrations in a total volume of 154 μL per well. In these conditions the initial fluorescence (F_0) was measured in all wells. Then a fixed concentration of peptide (10 μM) was added in each well, and the signal was recorded for 20 min. The fluorescence intensity after total leakage (F_{100}) was measured in all wells, after adding Triton X-100 (1 mM). Each measure was repeated three times using the following instrumental settings: $\lambda_{exc} = 450$ nm, $\lambda_{em} = 560$ nm, number of flashes = 25, integration time = 20 μs, settle time = 10 ms, lag time = 0 μs, mode = top, z position (manual) = 17750 μm, shaking mode = orbital, shaking duration = 3 s, shaking amplitude = 2.5 mm, number of kinetic cycles = 5. The temperature of instrument was set at 25 °C for all experiments. The gain was optimized for each liposome concentration in separate wells, where vesicles had been directly lysed by Triton addition, to obtain the maximum intensity value. The fraction of liposome contents released 20 min after peptide addition (RF) was determined as:

$$RF = \frac{F - F_0}{F_{100} - F_0}$$

2.4. Water-membrane partition experiments

Water-membrane partition experiments of P9-4 were performed on a Fluoromax 4 spectrofluorimeter (Horiba, Edison, NJ) and those of novicidin and Sub3 on a Fluoromax 2 spetrofluorimeter (Horiba, Edison, NJ). Experiments with P9-4 were repeated also using fluorescence anisotropy on a Fluoromax 4 spectrofluorimeter (Horiba, Edison, NJ) and fluorescence-lifetime on a Lifespec-ps (Edinburgh Instrument Ltd, Livingston, Scotland).

The membrane-bound peptide fraction (f_b) was calculated from the fluorescence intensity at fixed wavelengths (330, 340 and 305 nm for P9-4, Sub3 and novicidin, respectively) according to the following equation [16]:

$$f_b = \frac{(F - F_w)}{(F_m - F_w)}$$

where F_w and F_m represent the fluorescence intensities of the peptides in water and in the membrane, respectively. The latter was determined by fitting the following equation (describing the partition equilibrium), directly to the raw data (F vs $[L]$):

$$F = F_w + (F_m - F_w)\frac{\left(\frac{[L]}{K_d}\right)^n}{1 + \left(\frac{[L]}{K_d}\right)^n}$$

where $[L]$ and K_d represent the lipid concentrations and an apparent dissociation constant, while n is a parameter taking into account deviations from an ideal partition [40–41]. The above equation (which is derived from the well-known Hill equation) was used here only as a phenomenological description of the partition curve to enable extrapolation of the value of F_m. The other fitting parameters (K_d and n) were not further employed in our analysis, which is independent of a specific model for the partition equilibrium.

In fluorescence anisotropy and fluorescence lifetime experiments we used the same equation but replacing fluorescence intensities with fluorescence anisotropy and average fluorescence lifetime signals [23,40].

2.5. Steady-state fluorescence experiments

Steady-state fluorescence experiments were performed with a fixed peptide concentration (10 μM) and titrating with increasing lipid concentrations in a 10 mm × 4 mm fluorescence cuvette, exciting along the shorter path length. After each addition, the fluorescence spectra were recorded repeatedly until no further changes were observed (about 5–10 min). For P9-4, the following experimental conditions were employed: $\lambda_{exc} = 280$ nm, $\lambda_{em} = 300$–470 nm, integration time 0.4 s, bandwidth of 2 nm both in excitation and emission and a cut-off filter at 295 nm in the emission channel. For Sub 3 the conditions were $\lambda_{exc} = 280$ nm, $\lambda_{em} = 300$–470 nm, integration time 0.7 s, bandwidths of 2 and 2.5 nm in excitation and emission, respectively. In the case of novicidin, we used $\lambda_{exc} = 270$ nm, $\lambda_{em} = 290$–400 nm, integration time 1 s, bandwidths of 3 and 5 nm in excitation and emission. The temperature was controlled with a thermostatted cuvette holder set at 25 °C for all experiments. Control experiments to check for possible effects of sample turbidity on the fluorescence signal were performed by repeating the same titration with NATA (*N*-acetyl-L-tryptophan amide: Ac-Trp-NH_2), which demonstrated that no significant scattering artifacts were present (data not shown) [40].

2.6. Fluorescence anisotropy experiments

Fluorescence anisotropy experiments were performed with a fixed P9-4 concentration (10 μM) and titrating with increasing lipid concentrations in a fluorescence black bottom cuvette 10 mm × 4 mm, exciting along the shorter path length, using a magnetic stirrer and the following experimental conditions: $\lambda_{exc} = 280$ nm, $\lambda_{em} = 350$ nm, cut-off filter along the emission pathway at 305 nm, bandwidths of 4 and 5 nm in excitation and emission, respectively. The temperature was controlled with a thermostatted cuvette holder set to 25 °C for all experiments.

2.7. Time-resolved fluorescence experiments

Time-resolved fluorescence experiments for measuring peptide/membrane association were performed with the time-correlated single-photon counting technique in a LifeSpec-ps fluorometer (Edinburgh Instruments, UK). A fixed P9-4 concentration (10 μM) was titrated with increasing concentrations of liposomes in a fluorescence black-bottom cuvette, 10 mm × 4 mm, exciting along the shorter path length, using a magnetic stirrer, and the following experimental conditions: excitation with a pulsed light-emitting diode (Horiba NanoLED-280) with emission peaked at $\lambda_{exc} = 282$ nm, $\lambda_{em} = 350$ nm, cut-off filter in the emission channel at 305 nm, emission monochromator bandwidth = 8 nm, pulse repetition frequency = 1 MHz, acquisition time range = 50 ns, 1024 channels, 10.000 peak counts. The temperature was controlled with a

thermostatted cuvette holder set to 25 °C for all experiments. A biexponential curve was fitted to all fluorescence decays, and the values of the average lifetime were calculated from the two lifetimes and preexponential factors.

Time-resolved measurements were also employed to determine the leakage mechanism (all or none, or graded), according to [42]. In this case, vesicle leakage was induced by adding the peptide (at 10 μM final concentration) to a liposome suspension 37 μM in lipid. The process was stopped after different times (from 30 s to 5 min), when varying fractions of released dye had been reached in each sample (approx. in the range from 0.3 to 0.8 in the various samples). Leakage was stopped by addition of trypsin (to final concentration 75 μg/mL), which rapidly digested the peptide, and completely stopped the dye release within the few seconds needed for sample mixing (data not shown) [19]. Subsequently, the self-quenching of entrapped CF was determined by using time-resolved measurements. In this case, excitation was obtained with a pulsed diode laser (M89903-29, Hamamatsu Photonics K.K., Hamamatsu-City, Japan), with emission peaked at $\lambda_{exc} = 440$ nm (peak power 78 mW, pulse duration 95 ps (full width at half maximum). Emission was collected at $\lambda_{em} = 520$ nm, through a cut-off filter at 495 nm, using emission monochromator bandwidth = 16 nm. A biexponential function was fitted to the fluorescence decays, obtaining two lifetimes (corresponding to free and entrapped CF) and the relative preexponential factors.

3. Results

3.1. Only a fraction of vesicles is perturbed over a wide range of peptide to lipid ratios

The membrane-perturbing activity of the three peptides was studied by analyzing their interactions with synthetic vesicles. The simple binary POPE/POPG 7:3 mol/mol mixture represents the main components of many bacterial membranes, and therefore it is commonly used to mimic them: for instance, *E. coli* bilayers contain 70–80 % neutral (zwitterionic) phosphatidylethanolamine (PE) lipids, 10–20 % negatively charged phosphatidylglycerol (PG) lipids, and 5–15 % anionic cardiolipin [43–44]. While the membranes in bacteria are much more complex than these simple vesicles (for instance, due to the presence of proteins, or lipopolysaccharides), our goal was to verify and characterize the presence of a heterogeneous response to the action of peptides when studied in an extremely simplified system. Liposome leakage was determined as a function of the ratio between the (total) peptide concentration $[P]_{tot}$ (which was kept fixed) and the lipid concentration $[L]$ (which was varied). To this end, the peptide-induced release of a fluorophore entrapped inside vesicles at a self-quenching concentration was followed spectroscopically (Figs. S1 and 1A). Differences in the activities of the three peptides are apparent, with P9-4 being the least membrane-active (Fig. 1A). As expected, the released fraction of fluorophore increased with increasing $[P]_{tot}/[L]$. However, in an extremely wide range of $[P]_{tot}/[L]$ values (10^{-2} to 1, or 10 in the case of P9-4), only a fraction of the liposome contents was released, for all peptides investigated.

3.2. Leakage in vesicles is an "all or none" process

In principle, when a global leakage lower than 100 % is observed, two different scenarios are possible. In the so-called "all or none" mechanism, some vesicles are completely full, while others have released completely all their contents, or have been destroyed. In contrast, in the mechanism that has been termed "graded", all vesicles have released only part of their contents [45,16,19]. The behavior followed by a specific peptide depends on the time required for emptying a vesicle as compared to the lifetime of the peptide-induced pores [15]. For instance, if, once a pore is formed, a vesicle empties completely before the defect closes/heals, the "all or none" mechanism is a valid model. This is often the case for AMPs acting on large unilamellar vesicles (LUVs): simple calculations show that, in the case of 100 nm liposomes, the time required to empty a vesicle through a single peptide-induced pore is in the ms time range [15]. The mechanism can be defined experimentally by controlling the self-quenching efficiency of the fluorophore remaining inside the vesicles after partial leakage occurs. In the "all or none" mechanism, fluorescence remains self-quenched as in untreated vesicles, since a fraction of the vesicles is essentially unperturbed. In contrast, in the graded mechanism, the fluorophore concentration inside the vesicles decreases with an increased leaked fraction, and thus self-quenching is progressively reduced. The self-quenching efficiency can be tested by steady-state measurements [45,16,19] or by time-resolved experiments [42], which have the advantage of not requiring physical separation of the unentrapped dye. The fluorescence decay of the vesicle sample can usually be described by a biexponential decay, where the longer lifetime corresponds to the leaked, unquenched fluorophore, while the shorter lifetime is associated with the fluorophore still entrapped inside the vesicles. If the shorter lifetime does not change with the extent of global leakage, the mechanism is "all or none". Such experiments were performed on the three

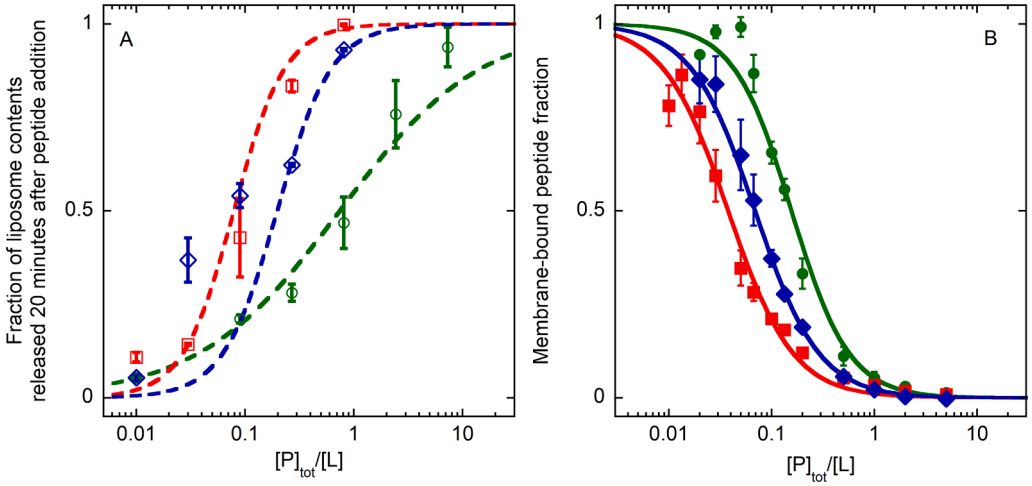

Fig. 1. Membrane-perturbing activity and membrane affinity of peptides. (A) Fraction of liposome contents (i.e., 5/6-carboxyfluorescein) released 20 min after peptide addition, as a function of the $\frac{[P]_{tot}}{[L]}$ ratio. (B) Membrane-bound peptide fraction, as a function of the $\frac{[P]_{tot}}{[L]}$ ratio. Green circles: P9-4; blue diamonds: Sub3; red squares: novicidin. (For interpretation of the references to color in this figure legend, the reader is referred to the web version of this article.).

peptides (Fig. 2) and demonstrate that this was indeed the case. Therefore, the partial leakage observed in Fig. 1 indicates that the AMPs caused the complete release of contents in some vesicles, leaving others completely unaffected.

Such heterogeneity in the response by individual liposomes under the same conditions is a common observation, which nonetheless is extremely puzzling. Significant differences between individual vesicles appear unlikely, due the narrow size distribution obtained by preparing liposomes by the extrusion method [15]. Another possible origin of heterogeneity is a variability in the number of peptides bound to each vesicle [15]. Simple geometrical considerations allow the calculation of the average number of lipids per vesicle in the $[P]_{tot}/[L]$ range 10^{-2} to 10. The total surface area (outer plus inner surface of the liposome) of a 100 nm diameter vesicle (formed by a bilayer about 4 nm thick) is approximately 6×10^4 nm^2. Considering that the area occupied by each lipid molecule is about 0.6 nm^2 [44], each vesicle is formed by $\sim 10^5$ lipid molecules. Therefore, in the $[P]_{tot}/[L]$ range investigated, $\sim 10^3$-10^6 peptide molecules were present per vesicle (at low versus high ratios). According to the Poisson distribution, these numbers should make vesicle-to-vesicle fluctuations in the number of bound peptides negligible (e.g., for 1000 bound peptides, the relative standard deviation would be 3 %).

3.3. Fluorescence spectroscopy allows the determination of the water-membrane partition equilibrium

Obviously, membrane perturbation is caused only by peptides bound to the liposomes. In order to consider the water-membrane partition equilibria of the three peptides, and thus the variation in the membrane-bound fraction with the lipid concentration, we characterized peptide association to liposomes. This was measured by following the change induced in the intrinsic fluorescence by the transition from the aqueous phase to the hydrophobic lipid environment (Figs. S2 and 1B): when the peptide binds to the membrane, its intrinsic fluorescence increases; in addition, for Trp-containing peptides, it shifts to shorter wavelengths. These data provide the membrane-bound peptide fraction as a function of the lipid concentration ($f_{bound}([L])$). For one of the peptides (P9-4) the

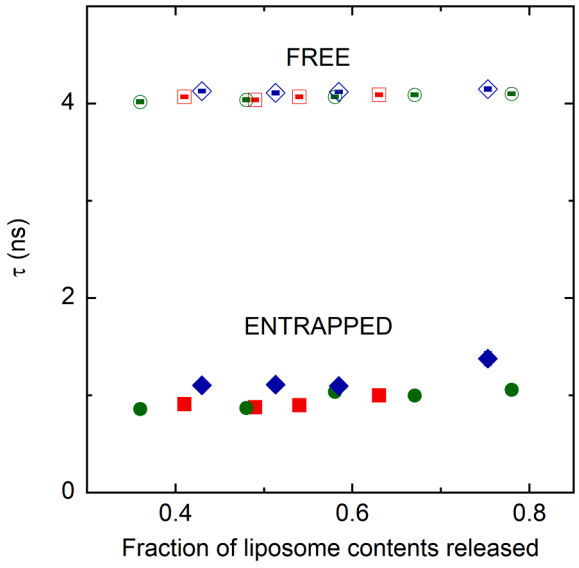

Fig. 2. CF fluorescence lifetimes after peptide-induced partial leakage of vesicles. Green circles: P9-4; blue diamonds: Sub3; red squares: novicidin. Full symbols: lifetimes of CF entrapped inside vesicles. Empty symbols: lifetimes of free dye. Peptide concentration = 10 μM. Lipid concentration: 37 μM. Vertical bars indicate the standard deviations on the lifetimes (as derived from the decay fits). (For interpretation of the references to color in this figure legend, the reader is referred to the web version of this article.).

partition isotherm was determined independently by two additional approaches (time-resolved fluorescence and emission anisotropy), and the three methods were in complete agreement (Fig. S3). Significant differences in membrane affinity were observed for the three peptides (Fig. 1B). Importantly, over the range of $[P]_{tot}/[L]$ (also used in the leakage experiments) the fraction of membrane-bound peptides varied from 0 to 1. Therefore, in this range, the concentration of peptide corresponding to the liposome-bound fraction ($[P]_{bound}$) was significantly different from the total peptide concentration ($[P]_{tot}$).

3.4. All vesicles are perturbed at a similar, well-defined critical threshold of membrane-bound peptide concentration

The peptide water/membrane partition data (Fig. 1B) allowed the calculation of $[P]_{bound}/[L]$ values under all experimental conditions used, and in particular at the $[P]_{tot}/[L]$ ratios used in the leakage experiments (Fig. S4), according to the following equation:

$$[P]_{bound}/[L] = [P]_{tot}/[L] \times f_{bound}([L])$$

When the leakage data are depicted as a function of the peptide fraction actually bound to the membranes (Fig. 3A), rather than as a function of the total peptide concentration, the curves become extremely steep, changing from a negligible perturbation to a total release within a very narrow range of $[P]_{bound}/[L]$ values. In fact, within the experimental error, the perturbation of all vesicles in the sample occurs around a critical threshold for $[P]_{bound}/[L]$. The specific $[P]_{bound}/[L]$ values resulting in leakage of liposome contents were approximately 2 % for novicidin and Sub3, and 6 % for P9-4. Due to the relatively large experimental errors on the data in Fig. 3 these values should be considered as order of magnitude estimates only. These findings show that, in terms of bound peptides, the transition from a state where all liposomes are unperturbed to a state where all vesicles release their contents, actually takes place at a well-defined threshold ratio, as expected for a system where all liposomes possess essentially identical physico-chemical properties.

3.5. When the peptide size is taken into account, the threshold ratio for pore formation is coincident for all peptides investigated

The threshold ratios (i.e., $[P]_{bound}/[L]$ values) for pore formation are somewhat different for the peptides investigated in the present study. This finding is not unexpected, since they differ in amino acid sequence, length and charge. To take into account at least the differences in length between the three AMPs, we plotted the fraction of liposome contents released as a function of membrane-bound amino acids, rather than bound peptide molecules (Fig. 3B). Rather surprisingly, in this case the threshold became even more similar for all three peptides, equal to 0.4 bound amino acids per lipid, suggesting that the mechanism of pore formation, once the peptides are inside the bilayer, is the same for all peptides investigated here.

4. Discussion and conclusion

The existence of a range of antimicrobial concentrations, where some bacteria are killed, while others survive is usually attributed to genetic differences between individual cells, leading to selection of resistant strains [6–8]. However, a similar behavior is observed even in clonal bacterial populations and in single-cell experiments, indicating that additional causes of heterogeneity must be at play [13]. For AMPs acting on bacterial membranes, a further level of simplification can be made, since their membrane activity can be approximated by testing on vesicles, identical in size and lipid composition. Nevertheless, even in this case, only a fraction of liposomes releases their contents over several orders of magnitude of peptide to lipid ratios [17–24].

The present findings demonstrate that the apparent heterogeneous response to AMPs actually arises from the water-membrane partition

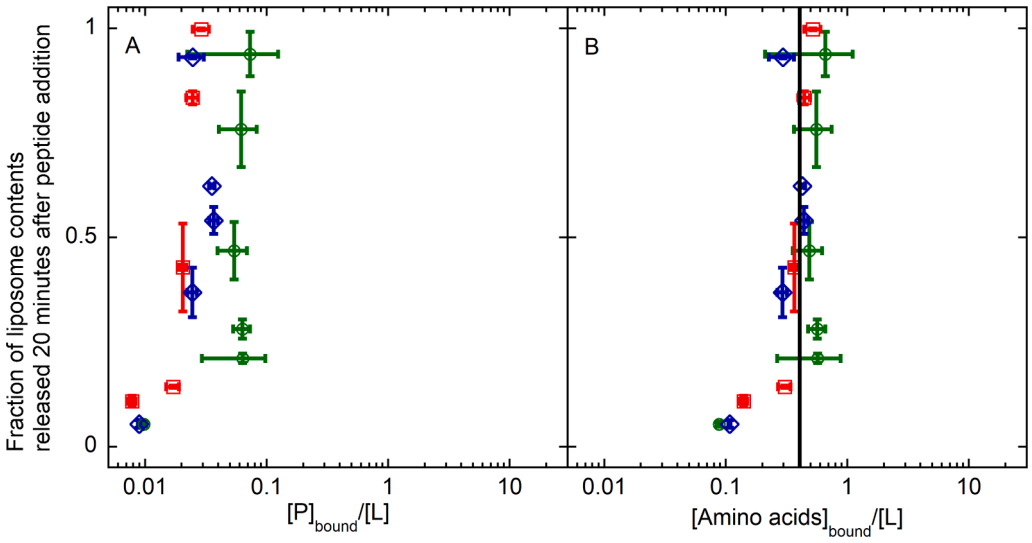

Fig. 3. Leakage curves reported as a function of the peptides or of the amino acids actually bound to the membranes rather than of the total peptide concentration. (A) Fraction of liposome contents released 20 min after peptide addition, as a function of the $\frac{[P]_{bound}}{[L]}$ ratio. (B) Fraction of liposome contents released 20 min after peptide addition, as a function of the $\frac{[Aminoacids]_{bound}}{[L]}$ ratio. Green circles: P9-4; blue diamonds: Sub3; red squares: novicidin. (For interpretation of the references to color in this figure legend, the reader is referred to the web version of this article.).

equilibrium of the peptides. When varying the lipid concentration $[L]$ (while keeping the peptide concentration fixed), the membrane-bound fraction of peptide f_b (that can form pores) is strongly affected, too [30,40,46]. For instance, in the simplest possible case of an ideal partition equilibrium, the fraction of membrane bound peptide can be expressed as $f_b = K_p[L]/[W]/(1+K_p[L]/[W])$, where K_p is the ideal partition constant, and $[W]$ is the concentration of pure water [17]. In this model, f_b depends on $[L]$ only, and when this variable is increased, f_b increases, too. Consequently, what appears to be a wide range of total peptide to lipid ratios, in fact corresponds to an extremely narrow range of bound peptide to lipid ratios. Hence, there exists a well-defined threshold for the bilayer-associated peptide content, which results in pore formation.

In other studies of AMP-induced pore formation, the lipid concentration was kept fixed, while the peptide concentration was varied. In this case, it was commonly observed that partial leakage occurred over a narrower range of total peptide to lipid ratios, that however still spanned about one order of magnitude [17–24]. In the ideal partition equilibrium discussed above, f_b depends on $[L]$ only, and therefore should be constant when the liposome concentration is kept constant. If this was the case, total and bound peptide would simply be proportional to each other, and the same heterogeneous response would be expected, regardless of the independent variable used in plotting the membrane activity of the peptide. However, non-ideal phenomena cannot be neglected. Incidentally, this is the reason why we used the phenomenological Hill equation reported in the methods section to extrapolate our data. In particular, water-membrane partition often depends on the peptide concentration, too [17,40]. Therefore, even in experiments performed at a constant lipid concentration, variations in the fraction of membrane-bound peptide may be invoked to explain the puzzling finding that the total AMP concentration causing complete leakage of all vesicles is significantly higher than the concentration, where initial liposome perturbation is observed. The variations in f_b when varying total peptide concentration, rather than total lipid concentration, can only be caused by non-idealities in the partition equilibrium, and therefore are expected to be smaller than those linked to changes in $[L]$, which directly affects the bound fraction. For instance, for the peptide DNS-PMAP23, we observed a variation in the apparent partition constant of just a factor of 2, when varying the peptide concentration tenfold [46]. Therefore, this interpretation also explains the different intervals of heterogeneous response observed in the two types of experiments.

Peptide-membrane association is an important determinant of membrane activity of AMPs against bacterial cells [30,40–41,46–47]. Our previous studies have indicated that water/membrane partition experiments performed on model vesicles represent a good model of the interaction of pore-forming AMPs with bacterial cells [40]. Therefore, the findings reported here constitute a relevant model for antimicrobial activity of AMPs, suggesting that partition between aqueous phase and membranes is an important phenomenon that is a contributing cause of the MSW. Even peptides that act intracellularly, rather than by forming pores (or via other membrane-disruptive processes), have an initial interaction with bacterial membranes in order to facilitate access to the cytosol. Therefore, water-membrane partition effects might be relevant also in these cases. However, *a priori* it is difficult to assess its significance as compared to genetic or phenotypic differences between cells. In this respect, a recent study demonstrated that even the heterogeneous AMP-sensitivity of individual bacteria that is caused by phenotypic differences, is mediated by differential peptide/membrane binding [14]. Experiments performed at high cell densities, where all the peptide molecules are bound to bacteria [30,40–41,46–47] may eliminate the partition effect, and allow for an evaluation of its relevance in causing the MSW. Quantification of peptide-cell binding is another possibility to verify the influence of this partition on the MSW.

The main strategy proposed to reduce the MSW is combination therapy with antibiotics having different modes of action. The basic idea behind this approach is that bacteria, which are not killed by one drug (due to their genetic or phenotypic properties) will be susceptible to the other antibacterial component(s) [48]. However, clinical experience shows that resistance may develop even during combination therapy [48]. Regarding the specific case of AMPs, it is important to note that in nature organisms usually synthetize several peptides [3]. Since the production of many AMPs is metabolically costly, this observation supports the advantage of combination therapy also in the case of these antimicrobials. Indeed, it has been shown that the combination of several AMPs does result in a reduced MSW, even when random mixtures of artificial peptides are employed, and even when all AMPs share the same mode of action (membrane perturbation) [7]. Consistently, AMP combinations have been demonstrated to hinder development of resistance as compared to the use of a single peptide, and the use of random combinatorial AMP libraries (containing more than 1 million

sequences) resulted in no detectable resistance [10–11]. Specific effects might be at play, too, since several AMP combinations exhibit synergy [3], and it has been shown that synergistic combinations have a narrower MSW than the individual peptides [9]. While the mechanism of synergy is debated, it is interesting to note that in the specific case of magainin and PGLa, synergy and MSW narrowing are accompanied by an increased membrane binding of the peptides [9,49], so that water-membrane partition could play a role in this case too.

The findings presented here indicate an additional possible strategy to reduce the MSW, by predicting that AMPs with a high affinity towards bacterial membranes will have a narrower MSW. For such AMPs most peptide molecules will be bound to bacteria under the standard conditions used in susceptibility assays or present in clinically relevant infections. Therefore, total and bound peptide concentrations will coincide, and the effect of water-membrane partition on the MSW will be eliminated. Peptides with high membrane affinity would be desirable also because a higher membrane-bound fraction would result in higher activity. Unfortunately, it must be considered that decades of experience with rational design of AMPs have shown that the driving forces for peptide-membrane binding (electrostatic attraction, and hydrophobic effect) can be increased only up to a certain point without compromising activity and cell selectivity [43]. For instance, a peptide that is too highly charged may remain on the surface without causing extensive perturbation, while excessively hydrophobic peptides usually become toxic to the host cells [43].

Our data showed that the thresholds for pore formation coincide for the three AMPs investigated, in terms of bound amino acids per lipid. In general, the membrane activity of a specific AMP depends at least on two phenomena: how efficiently it binds to lipid bilayers, and its ability to perturb them once it becomes inserted. By determining the membrane-bound peptide concentration, we separated these two effects. Membrane affinity can be determined in water-membrane partition studies, and it is strongly influenced by the peptide sequence, particularly by the overall charge and hydrophobicity. The specific amino acid composition of an AMP can also affect its location and depth of penetration into the bilayer, and thus influence its membrane-perturbing effects. The threshold of membrane-bound peptide causing pore formation, as determined in the present study, quantifies the second aspect, i.e., the bilayer-destabilizing ability of an AMP. The fact that the three peptides investigated here share a similar threshold might arise from a similar charge density (Table 1). In any case, this finding provides strong support for the so-called “carpet” mechanism of pore formation [50]. According to this model, formation of defects in the bilayer is caused by the perturbation of the surface tension of the outer leaflet, due to the accumulation of peptides below the lipid head groups [40]. Therefore, AMPs act essentially by a mechanism, where the bulk of the inserted peptides perturbs the packing of the lipid tails. The specific sequence and physico-chemical properties of each peptide determine its affinity for the membrane, selectivity for different lipid compositions, and depth of insertion into the bilayer [43]. However, once the AMPs are membrane-bound at a proper depth, only the total volume of accumulated peptide determines the threshold required for pore formation. Incidentally, in this picture the slightly lower activity of P9-4, compared to the other peptides (Fig. 1A) can be explained by its smaller size (Table 1). The threshold identified here (approximately 0.4 amino acids per lipid) corresponds to a high coverage of the membrane surface, as predicted by the carpet model, and demonstrated experimentally by our previous studies on peptide/cell interactions [30,40–41,46–47]. Our data on the cell-density dependence of the activity of peptides [30,46] indicated that this state always requires micromolar concentrations of AMPs, even at very low bacterial cell densities. Some exceptions of AMPs active in the nM range do exist [51–52]. However, an analysis of the GRAMPA database (Giant Repository of AMP Activities) [53] showed that activities below 0.1 μM account for less than 2 % of the minimum inhibitory concentration (MIC) data in the database, and in many cases are related to peptides that act on specific targets (rather than on membranes). Therefore, the questions might arise whether these conditions are attainable in vivo. Micromolar concentrations are reached physiologically in the granules of leukocytes, on the skin of frogs, and in the hemolymph of infected insects [30,43,54–55]. In addition, most animal hosts elicit the production of several AMPs, often acting synergistically, lowering the required concentration of each peptide in the mixture. Where the physiological concentrations of AMPs are lower than the threshold values for pore formation, other functions, particularly immunomodulation, might be more important than direct bacterial killing.

CRediT authorship contribution statement

Federico Carneri: Writing – review & editing, Writing – original draft, Visualization, Software, Investigation, Formal analysis, Data curation. **Cassandra Troiano:** Writing – review & editing, Methodology, Investigation, Data curation. **Giuseppe Giaquinto:** Writing – review & editing, Investigation, Formal analysis, Data curation. **Daniela Roversi:** Writing – review & editing, Visualization, Investigation, Data curation. **Henrik Franzyk:** Writing – review & editing, Resources, Methodology. **Lorenzo Stella:** Writing – review & editing, Writing – original draft, Visualization, Supervision, Resources, Methodology, Funding acquisition, Data curation, Conceptualization.

Funding

This work was supported by the Italian Ministry for University (grant PRIN 2020833Y75_005 and grant PNRR M4C2I1.3-HEAL ITALIA project PE 00000019) to L.S., Dipartimento di Eccellenza 2023–27 X-CHEM project, to the Department of Chemical Science and Technologies, Tor Vergata University of Rome).

Declaration of competing interest

The authors declare that they have no known competing financial interests or personal relationships that could have appeared to influence the work reported in this paper.

Appendix A. Supplementary data

Supplementary data to this article can be found online at https://doi.org/10.1016/j.jcis.2024.12.099.

Data availability

Data will be made available on request.

References

[1] T.R. Walsh, A.C. Gales, R. Laxminarayan, P.C. Dodd, Antimicrobial Resistance: Addressing a Global Threat to Humanity, PLoS Med. 20 (7) (2023) e1004264, https://doi.org/10.1371/journal.pmed.1004264.

[2] C.J.L. Murray, K.S. Ikuta, F. Sharara, L. Swetschinski, G. Robles Aguilar, A. Gray, C. Han, C. Bisignano, P. Rao, E. Wool, S.C. Johnson, A.J. Browne, M.G. Chipeta, F. Fell, S. Hackett, G. Haines-Woodhouse, B.H. Kashef Hamadani, E.A.P. Kumaran, B. McManigal, S. Achalapong, R. Agarwal, S. Akech, S. Albertson, J. Amuasi, J. Andrews, A. Aravkin, E. Ashley, F.-X. Babin, F. Bailey, S. Baker, B. Basnyat, A. Bekker, R. Bender, J.A. Berkley, A. Bethou, J. Bielicki, S. Boonkasidecha, J. Bukosia, C. Carvalheiro, C. Castañeda-Orjuela, V. Chansamouth, S. Chaurasia, S. Chiurchiù, F. Chowdhury, R. Clotaire Donatien, A.J. Cook, B. Cooper, T. R. Cressey, E. Criollo-Mora, M. Cunningham, S. Darboe, N.P.J. Day, M. De Luca, K. Dokova, A. Dramowski, S.J. Dunachie, T. Duong Bich, T. Eckmanns, D. Eibach, A. Emami, N. Feasey, N. Fisher-Pearson, K. Forrest, C. Garcia, D. Garrett, P. Gastmeier, A.Z. Giref, R.C. Greer, V. Gupta, S. Haller, A. Haselbeck, S.I. Hay, M. Holm, S. Hopkins, Y. Hsia, K.C. Iregbu, J. Jacobs, D. Jarovsky, F. Javanmardi, A. W.J. Jenney, M. Khorana, S. Khusuwan, N. Kissoon, E. Kobeissi, T. Kostyanev, F. Krapp, R. Krumkamp, A. Kumar, H.H. Kyu, C. Lim, K. Lim, D. Limmathurotsakul, M.J. Loftus, M. Lunn, J. Ma, A. Manoharan, F. Marks, J. May, M. Mayxay, N. Mturi, T. Munera-Huertas, P. Musicha, L.A. Musila, M.M. Mussi-Pinhata, R.N. Naidu, T. Nakamura, R. Nanavati, S. Nangia, P. Newton, C. Ngoun, A. Novotney, D. Nwakanma, C.W. Obiero, T.J. Ochoa, A. Olivas-Martinez, P. Olliaro, E. Ooko,

E. Ortiz-Brizuela, P. Ounchanum, G.D. Pak, J.L. Paredes, A.Y. Peleg, C. Perrone, T. Phe, K. Phommasone, N. Plakkal, A. Ponce-de-Leon, M. Raad, T. Ramdin, S. Rattanavong, A. Riddell, T. Roberts, J.V. Robotham, A. Roca, V.D. Rosenthal, K. E. Rudd, N. Russell, H.S. Sader, W. Saengchan, J. Schnall, J.A.G. Scott, S. Seekaew, M. Sharland, M. Shivamallappa, J. Sifuentes-Osornio, A.J. Simpson, N. Steenkeste, A.J. Stewardson, T. Stoeva, N. Tasak, A. Thaiprakong, G. Thwaites, C. Tigoi, C. Turner, P. Turner, H.R. van Doorn, S. Velaphi, A. Vongpradith, M. Vongsouvath, H. Vu, T. Walsh, J.L. Walson, S. Waner, T. Wangrangsimakul, P. Wannapinij, T. Wozniak, T.E.M.W. Young Sharma, K.C. Yu, P. Zheng, B. Sartorius, A.D. Lopez, A. Stergachis, C. Moore, C. Dolecek, M. Naghavi, Global Burden of Bacterial Antimicrobial Resistance in 2019: A Systematic Analysis, Lancet 399 (10325) (2022) 629–655, https://doi.org/10.1016/s0140-6736(21)02724-0.

[3] B.P. Lazzaro, M. Zasloff, J. Rolff, Antimicrobial Peptides: Application Informed by Evolution, Science 368 (6490) (2020) eaau5480, https://doi.org/10.1126/science.aau5480.

[4] G. Yu, D.Y. Baeder, R.R. Regoes, J. Rolff, Predicting Drug Resistance Evolution: Insights from Antimicrobial Peptides and Antibiotics, Proc. Biol. Sci. 285 (1874) (2018) 20172687, https://doi.org/10.1098/rspb.2017.2687.

[5] J.A. Roberts, P. Kruger, D.L. Paterson, J. Lipman, Antibiotic Resistance—What's Dosing Got to Do with It? Crit. Care Med. 36 (8) (2008) 2433–2440, https://doi.org/10.1097/ccm.0b013e318180fe62.

[6] K. Drlica, X. Zhao, Mutant Selection Window Hypothesis Updated, Clin. Infect. Dis. 44 (5) (2007) 681–688, https://doi.org/10.1086/511642.

[7] G. Yu, D.Y. Baeder, R.R. Regoes, J. Rolff, Combination Effects of Antimicrobial Peptides, Antimicrob. Agents Chemother. 60 (3) (2016) 1717–1724, https://doi.org/10.1128/aac.02434-15.

[8] B. El Shazely, G. Yu, P.R. Johnston, J. Rolff, Resistance Evolution against Antimicrobial Peptides in Staphylococcus aureus Alters Pharmacodynamics beyond the MIC, Front. Microbiol. 11 (2020) 103, https://doi.org/10.3389/fmicb.2020.00103.

[9] B. Bechinger, D.W. Juhl, E. Glattard, C. Aisenbrey, Revealing the Mechanisms of Synergistic Action of Two Magainin Antimicrobial Peptides, Front. Med. Technol. 2 (2020) 615494, https://doi.org/10.3389/fmedt.2020.615494.

[10] B. Maron, J. Rolff, J. Friedman, Z. Hayouka, Antimicrobial Peptide Combination can Hinder Resistance Evolution, Microbiol. Spectr. 10 (4) (2022) e00973–e01022, https://doi.org/10.1128/spectrum.00973-22.

[11] B. Antunes, C. Zanchi, P.R. Johnston, B. Maron, C. Witzany, R.R. Regoes, J. Rolff, The Evolution of Antimicrobial Peptide Resistance in Pseudomonas aeruginosa is Severely Constrained by Random Peptide Mixtures, PLOS Biol. 22 (7) (2024) e3002692, https://doi.org/10.1371/journal.pbio.3002692.

[12] M. Costa, C. Meirinhos, E. Cunha, D. Gomes, M. Pereira, R. Dias, L. Tavares, M. Oliveira, Nisin Mutant Prevention Concentration and the Role of Subinhibitory Concentrations on Resistance Development by Diabetic Foot Staphylococci, Antibiotics (Basel) 11 (7) (2022) 972, https://doi.org/10.3390/antibiotics11070972.

[13] J. Cama, K. Al Nahas, M. Fletcher, K. Hammond, M.G. Ryadnov, U.F. Keyser, S. Pagliara, An Ultrasensitive Microfluidic Approach Reveals Correlations between the Physico-Chemical and Biological Activity of Experimental Peptide Antibiotics, Sci. Rep. 12 (1) (2022) 4005, https://doi.org/10.1038/s41598-022-07973-z.

[14] K.K. Lee, U. Łapińska, G. Tolle, W. Phetsang, A.D. Verderosa, B.M. Invergo, J. Westley, A. Bebes, R. Yuecel, P.A. O'Neill, A. Farbos, A.R. Jeffries, S. van Houte, P. Caboni, M.A.T. Blaskovice, B.E. Housden, K. Tsaneva-Atanasova, S. Pagliara, Heterogeneous Efflux Pump Expression Underpins Phenotypic Resistance to Antimicrobial Peptides, eLife (2024), https://doi.org/10.7554/eLife.99752.1.

[15] C. Mazzuca, B. Orioni, M. Coletta, F. Formaggio, C. Toniolo, G. Maulucci, M. De Spirito, B. Pispisa, M. Venanzi, L. Stella, Fluctuations and the Rate-Limiting Step of Peptide-Induced Membrane Leakage, Biophys. J. 99 (6) (2010) 1791–1800, https://doi.org/10.1016/j.bpj.2010.07.010.

[16] G. Bocchinfuso, S. Bobone, C. Mazzuca, A. Palleschi, L. Stella, Fluorescence Spectroscopy and Molecular Dynamics Simulations in Studies on the Mechanism of Membrane Destabilization by Antimicrobial Peptides, Cell. Mol. Life Sci. 68 (13) (2011) 2281–2301, https://doi.org/10.1007/s00018-011-0719-1.

[17] L. Stella, C. Mazzuca, M. Venanzi, A. Palleschi, M. Didonè, F. Formaggio, C. Toniolo, B. Pispisa, Aggregation and Water-Membrane Partition as Major Determinants of the Activity of the Antibiotic Peptide Trichogin GA IV, Biophys. J. 86 (2) (2004) 936–945, https://doi.org/10.1016/s0006-3495(04)74169-7.

[18] C. Mazzuca, L. Stella, M. Venanzi, F. Formaggio, C. Toniolo, B. Pispisa, Mechanism of Membrane Activity of the Antibiotic Trichogin GA IV: A Two-State Transition Controlled by Peptide Concentration, Biophys. J. 88 (5) (2005) 3411–3421, https://doi.org/10.1529/biophysj.104.056077.

[19] B. Orioni, G. Bocchinfuso, J.Y. Kim, A. Palleschi, G. Grande, S. Bobone, Y. Park, J. I. Kim, K.-S. Hahm, L. Stella, Membrane Perturbation by the Antimicrobial Peptide PMAP-23: A Fluorescence and Molecular Dynamics Study, Biochim. Biophys. Acta 1788 (7) (2009) 1523–1533, https://doi.org/10.1016/j.bbamem.2009.04.013.

[20] S. Bobone, D. Roversi, L. Giordano, M. De Zotti, F. Formaggio, C. Toniolo, Y. Park, L. Stella, The Lipid Dependence of Antimicrobial Peptide Activity Is an Unreliable Experimental Test for Different Pore Models, Biochemistry 51 (51) (2012) 10124–10126, https://doi.org/10.1021/bi3015086.

[21] S. Bobone, G. Bocchinfuso, Y. Park, A. Palleschi, K.-S. Hahm, L. Stella, The Importance of Being Kinked: Role of Pro Residues in the Selectivity of the Helical Antimicrobial Peptide P5, J. Pept. Sci. 19 (12) (2013) 758–769, https://doi.org/10.1002/psc.2574.

[22] Z. Vaezi, A. Bortolotti, V. Luca, G. Perilli, M.L. Mangoni, R. Khosravi-Far, S. Bobone, L. Stella, Aggregation Determines the Selectivity of Membrane-Active Anticancer and Antimicrobial Peptides: The Case of killerFLIP, Biochim. Biophys. Acta Biomembr. 1862 (2) (2020) 183107, https://doi.org/10.1016/j.bbamem.2019.183107.

[23] S. Bobone, C. Storti, P. Calligari, L. Stella, Fluorescence Anisotropy and Polarization in the Characterization of Biomolecular Association Processes and Their Application to Study SH2 Domain Binding Affinity, Methods Mol. Biol. 2705 (2023) 93–112, https://doi.org/10.1007/978-1-0716-3393-9_6.

[24] D. Roversi, C. Troiano, E. Salnikov, L. Giordano, F. Riccitelli, M. De Zotti, B. Casciaro, M.R. Loffredo, Y. Park, F. Formaggio, M.L. Mangoni, B. Bechinger, L. Stella, Effects of Antimicrobial Peptides on Membrane Dynamics: A Comparison of Fluorescence and NMR Experiments, Biophys. Chem. 300 (107060) (2023) 107060, https://doi.org/10.1016/j.bpc.2023.107060.

[25] V.S. Balakrishnan, B.S. Vad, D.E. Otzen, Novicidin's Membrane Permeabilizing Activity Is Driven by Membrane Partitioning but Not by Helicity: A Biophysical Study of the Impact of Lipid Charge and Cholesterol, Biochim. Biophys. Acta 1834 (6) (2013) 996–1002, https://doi.org/10.1016/j.bbapap.2013.03.025.

[26] C.T. Gottlieb, L.E. Thomsen, H. Ingmer, P.H. Mygind, H.-H. Kristensen, L. Gram, Antimicrobial Peptides Effectively Kill a Broad Spectrum of Listeria Monocytogenes and Staphylococcus Aureus Strains Independently of Origin, Sub-Type, or Virulence Factor Expression, BMC Microbiol. 8 (2008) 205, https://doi.org/10.1186/1471-2180-8-205.

[27] S.B. Nielsen, D.E. Otzen, Impact of the Antimicrobial Peptide Novicidin on Membrane Structure and Integrity, J. Colloid Interface Sci. 345 (2) (2010) 248–256, https://doi.org/10.1016/j.jcis.2010.01.065.

[28] J. Dorosz, Y. Gofman, S. Kolusheva, D. Otzen, N. Ben-Tal, N.C. Nielsen, R. Jelinek, Membrane Interactions of Novicidin, a Novel Antimicrobial Peptide: Phosphatidylglycerol Promotes Bilayer Insertion, J. Phys. Chem. B 114 (34) (2010) 11053–11060, https://doi.org/10.1021/jp1052248.

[29] X. Qi, C. Zhou, P. Li, W. Xu, Y. Cao, H. Ling, W. Ning Chen, C. Ming Li, R. Xu, M. Lamrani, Y. Mu, S.S.J. Leong, M. Wook Chang, M.B. Chan-Park, Novel Short Antibacterial and Antifungal Peptides with Low Cytotoxicity: Efficacy and Action Mechanisms, Biochem. Biophys. Res. Commun. 398 (3) (2010) 594–600, https://doi.org/10.1016/j.bbrc.2010.06.131.

[30] M.R. Loffredo, F. Savini, S. Bobone, B. Casciaro, H. Franzyk, M.L. Mangoni, L. Stella, Inoculum Effect of Antimicrobial Peptides, Proc. Natl. Acad. Sci. U. S. A. 118 (21) (2021) e2014364118, https://doi.org/10.1073/pnas.2014364118.

[31] K. Hilpert, R. Volkmer-Engert, T. Walter, R.E.W. Hancock, High-Throughput Generation of Small Antibacterial Peptides with Improved Activity, Nat. Biotechnol. 23 (8) (2005) 1008–1012, https://doi.org/10.1038/nbt1113.

[32] K. Hilpert, B. McLeod, J. Yu, M.R. Elliott, M. Rautenbach, S. Ruden, J. Bürck, C. Muhle-Goll, A.S. Ulrich, S. Keller, R.E.W. Hancock, Short Cationic Antimicrobial Peptides Interact with ATP, Antimicrob. Agents Chemother. 54 (10) (2010) 4480–4483, https://doi.org/10.1128/aac.01664-09.

[33] D. Knappe, P. Henklein, R. Hoffmann, K. Hilpert, Easy Strategy to Protect Antimicrobial Peptides from Fast Degradation in Serum, Antimicrob. Agents Chemother. 54 (9) (2010) 4003–4005, https://doi.org/10.1128/AAC.00300-10.

[34] I.M. Torcato, Y.-H. Huang, H.G. Franquelim, D.D. Gaspar, D.J. Craik, M.A.R. B. Castanho, S.T. Henriques, The Antimicrobial Activity of Sub3 Is Dependent on Membrane Binding and Cell-Penetrating Ability, Chembiochem 14 (15) (2013) 2013–2022, https://doi.org/10.1002/cbic.201300274.

[35] A.M. Hansen, G. Bonke, C.J. Larsen, N. Yavari, P.E. Nielsen, H. Franzyk, Antibacterial Peptide Nucleic Acid-Antimicrobial Peptide (PNA-AMP) Conjugates: Antisense Targeting of Fatty Acid Biosynthesis, Bioconjug. Chem. 27 (4) (2016) 863–867, https://doi.org/10.1021/acs.bioconjchem.6b00013.

[36] K.R. Baker, B. Jana, A.M. Hansen, K.J. Vissing, H.M. Nielsen, H. Franzyk, L. Guardabassi, Repurposing Azithromycin and Rifampicin against Gram-negative Pathogens by Combination with Peptide Potentiators, Int. J. Antimicrob. Agents 53 (6) (2019) 868–872, https://doi.org/10.1016/j.ijantimicag.2018.10.025.

[37] A. Bortolotti, C. Troiano, S. Bobone, M.M. Konai, C. Ghosh, G. Bocchinfuso, Y. Acharya, V. Santucci, S. Bonacorsi, C. Di Stefano, J. Haldar, L. Stella, Mechanism of Lipid Bilayer Perturbation by Bactericidal Membrane-Active Small Molecules, Biochim. Biophys. Acta Biomembr. 1865 (1) (2023) 184079, https://doi.org/10.1016/j.bbamem.2022.184079.

[38] J.C. Stewart, Colorimetric Determination of Phospholipids with Ammonium Ferrothiocyanate, Anal. Biochem. 104 (1) (1980) 10–14, https://doi.org/10.1016/0003-2697(80)90269-9.

[39] R.F. Chen, J.R. Knutson, Mechanism of Fluorescence Concentration Quenching of Carboxyfluorescein in Liposomes: Energy Transfer to Nonfluorescent Dimers, Anal. Biochem. 172 (1) (1988) 61–77, https://doi.org/10.1016/0003-2697(88)90412-5.

[40] D. Roversi, V. Luca, S. Aureli, Y. Park, M.L. Mangoni, L. Stella, How Many Antimicrobial Peptide Molecules Kill a Bacterium? The Case of PMAP-23, ACS Chem. Biol. 9 (9) (2014) 2003–2007, https://doi.org/10.1021/cb500426r.

[41] F. Savini, M.R. Loffredo, C. Troiano, S. Bobone, N. Malanovic, T.O. Eichmann, L. Caprio, V.C. Canale, Y. Park, M.L. Mangoni, L. Stella, Binding of an Antimicrobial Peptide to Bacterial Cells: Interaction with Different Species, Strains and Cellular Components, Biochim. Biophys. Acta Biomembr. 1862 (8) (2020) 183291, https://doi.org/10.1016/j.bbamem.2020.183291.

[42] H. Patel, C. Tscheka, H. Heerklotz, Characterizing Vesicle Leakage by Fluorescence Lifetime Measurements, Soft Matter 5 (15) (2009) 2849, https://doi.org/10.1039/b908524f.

[43] S. Bobone, L. Stella, Selectivity of Antimicrobial Peptides: A Complex Interplay of Multiple Equilibria, Advances in Experimental Medicine and Biology 1117 (2019) 175–214, https://doi.org/10.1007/978-981-13-3588-4_11.

[44] K. Murzyn, T. Róg, M. Pasenkiewicz-Gierula, Phosphatidylethanolamine-Phosphatidylglycerol Bilayer as a Model of the Inner Bacterial Membrane, Biophys. J. 88 (2) (2005) 1091–1103, https://doi.org/10.1529/biophysj.104.048835.

[45] A.S. Ladokhin, W.C. Wimley, K. Hristova, S.H. White, Mechanism of Leakage Contents of Membrane Vesicles Determined by Fluorescence Requenching, Methods Enzymol 278 (1997) 474–486.
[46] F. Savini, V. Luca, A. Bocedi, R. Massoud, Y. Park, M.L. Mangoni, L. Stella, Cell-Density Dependence of Host-Defense Peptide Activity and Selectivity in the Presence of Host Cells, ACS Chem. Biol. 12 (1) (2017) 52–56, https://doi.org/10.1021/acschembio.6b00910.
[47] F. Savini, S. Bobone, D. Roversi, M.L. Mangoni, L. Stella, From Liposomes to Cells: Filling the Gap between Physicochemical and Microbiological Studies of the Activity and Selectivity of Host-defense Peptides, Pept. Sci. (Hoboken) 110 (5) (2018) e24041, https://doi.org/10.1002/pep2.24041.
[48] X. Zhao, K. Drlica, Restricting the Selection of Antibiotic-resistant Mutants: a General Strategy Derived from Fluoroquinolone Studies, Clin. Infect. Dis. 33 (Supplement_3) (2001) S147–S156, https://doi.org/10.1086/321841.
[49] C. Aisenbrey, M. Amaro, P. Pospíšil, M. Hof, B. Bechinger, Highly Synergistic Antimicrobial Activity of Magainin 2 and PGLa Peptides is Rooted in the Formation of Supramolecular Complexes with Lipids, Sci. Rep. 10 (1) (2020) 11652, https://doi.org/10.1038/s41598-020-68416-1.
[50] Y. Shai, Mode of Action of Membrane Active Antimicrobial Peptides, Biopolymers 66 (4) (2002) 236–248, https://doi.org/10.1002/bip.10260.
[51] V. Frecer, B. Ho, D.J.L. De, novo Design of Potent Antimicrobial Peptides, Antimicrob. Agents. Chemother. 48 (9) (2004) 3349–3357, https://doi.org/10.1128/aac.48.9.3349-3357.2004.
[52] K. Hammond, J. Moffat, C. Mulcahy, B.W. Hoogenboom, M.G. Ryadnov, In situ Nanoscale Imaging Reveals Self-concentrating Nanomolar Antimicrobial Pores, Nanoscale 14 (24) (2022) 8586–8593, https://doi.org/10.1039/D2NR00434H.
[53] J. Witten, Z. Witten, Deep Learning Regression Model for Antimicrobial Peptide Design, BioRxiv 692681 (2019), https://doi.org/10.1101/692681.
[54] B. Lemaitre, J. Hoffmann, The Host Defense of Drosophila melanogaster, Annu. Rev. Immunol. 25 (1) (2007) 697–743, https://doi.org/10.1146/annurev.immunol.25.022106.141615.
[55] O.Makarova, A. Rodriguez-Rojas, M. Eravci, C. Weise, A. Dobson, P. Johnston, J. Rolff, Antimicrobial Defence and Persistent Infection in Insects Revisited. Philos. Trans. R Soc. Lond. B Biol. Sci. 371 (1695) (2016) 20150296, doi: 10.1098/rstb.2015.0296. Corrected in: Philos. Trans. R Soc. Lond. B Biol. Sci. 371 (1699) (2016) 20160263, doi: 10.1098/rstb.2016.0263.

Glossary

AMP: antimicrobial peptide
AMR: antimicrobial resistance
CF: 5(6)-Carboxyfluorescein
DIC: diisopropylcarbodiimide
DMF: dimethylformamide
EDTA: ethylenediaminetetraacetic acid
GRAMPA: Giant Repository of AMP Activities
LUVs: large unilamellar vesicles
MeCN: acetonitrile
MeOH: methanol
MIC: minimum inhibitory concentration
MSW: mutant selection window
NATA: N-acetyl-L-tryptophan amide
PE: phosphatidylethanolamine
PG: phosphatidylglycerol
POPE: 1-palmitoyl-2-oleoyl-*sn*-glycero-3-phosphatidylethanolamine
POPG: 1-palmitoyl-2-oleoyl-*sn*-glycero-3-phospho-(1′-*rac*-glycerol)
TFA: trifluoroacetic acid
Trp: L-tryptophan.

SUPPORTING INFORMATION

Water-membrane partition and the mutant selection window of antimicrobial peptides: insights from liposome studies

Federico Carneri,[a,b] *Cassandra Troiano,*[a] *Giuseppe Giaquinto,*[a] *Daniela Roversi,*[a] *Henrik Franzyk,*[c] *Lorenzo Stella.*[a,*]

[a] Department of Chemical Science and Technologies, Tor Vergata University of Rome, 00133 Rome, Italy.

[b] Photoinduced Processes and Technologies Doctoral School, Perugia University, 06123 Perugia, Italy.

[c] Department of Drug Design and Pharmacology, University of Copenhagen, DK-2100 Copenhagen, Denmark.

* To whom correspondence should be addressed. Prof. Lorenzo Stella. Department of Chemical Science and Technologies, Tor Vergata University of Rome, Via della ricerca scientifica, 1, 00133, Rome, Italy. stella@stc.uniroma2.it.

Table S1. Characterization of peptide purity

Name	Molecular weight (including TFA)	Purity	HPLC retention time (min.)
Novicidin	3322.09	95%	10.41
P9-4	1968.85	98%	10.44
Sub3	2462.26	99%	8.50

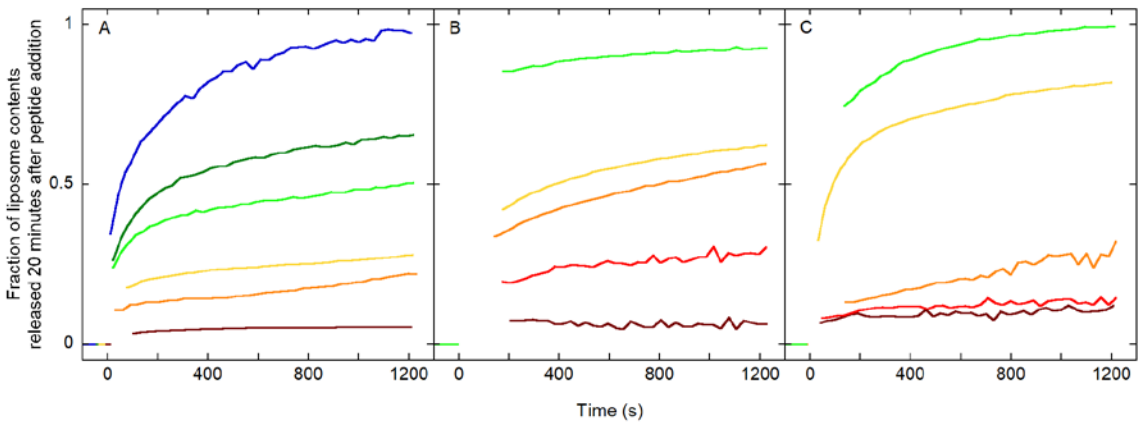

Figure S1. Kinetics of peptide-induced membrane leakage.

(A) P9-4; (B) Sub3; (C) Novicidin. The kinetic tracers are colored from red to blue with decreasing lipid concentration. Peptide concentration = 10 μM. Lipid concentrations: $1.0 \cdot 10^3$ μM (dark red) $1.1 \cdot 10^2$ μM (orange), 37 μM (yellow), 12 μM (light green), 4.1 μM (green), 1.4 μM (blue) for P9-4 (A); $1.0 \cdot 10^3$ μM (dark red), $3.3 \cdot 10^2$ μM (red), $1.1 \cdot 10^2$ μM (orange), 37 μM (yellow), 12 μM (light green) for Sub3 (B) and Novicidin (C).

The curves reported in the plot are representative of measurements repeated in triplicate.

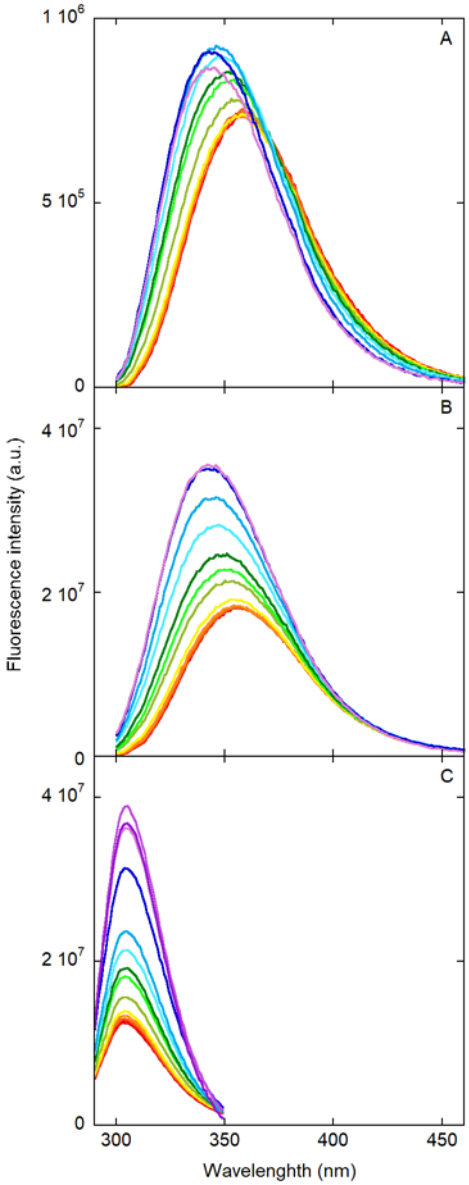

Figure S2. Emission spectra of peptides in the presence of increasing lipid concentrations. Spectra are colored from red to violet with increasing lipid concentration. (A) P9-4; (B) Sub3; (C) Novicidin. Peptide concentration = 10 μM; Lipid concentrations: 0, 2.0, 5.0, 10, 20, 50, 75, 1.0×10^2, 1.5×10^2, 2.0×10^2, 3.5×10^2, 5.0×10^2 μM for P9-4 (A) and Sub3 (B). Lipid concentrations: 0, 2.0, 5.0, 10, 20, 50, 75, 1.0×10^2, 1.5×10^2, 2.0×10^2, 3.5×10^2, 5.0×10^2, 7.5×10^2, 1.0×10^3 μM for novicidin (C). The spectra reported in the plot are representative of measurements repeated in triplicate.

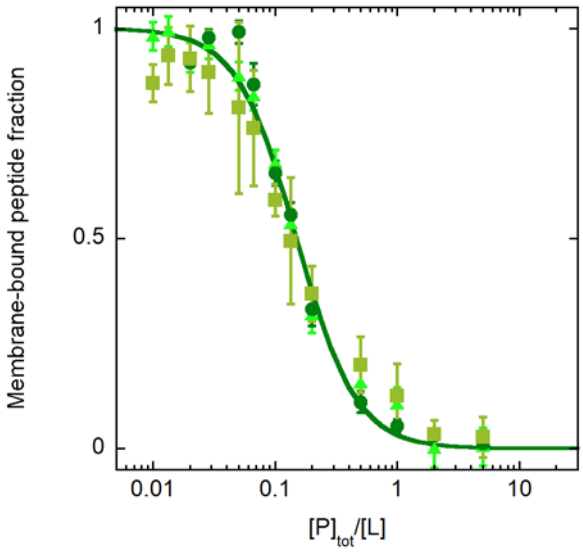

Figure S3. Comparison of membrane-bound P9-4 fractions as a function of increasing lipid concentration obtained with three different spectroscopic techniques.

Circles: steady-state fluorescence; squares: fluorescence anisotropy; triangles: time-resolved fluorescence. P9-4 concentration: 10 µM.

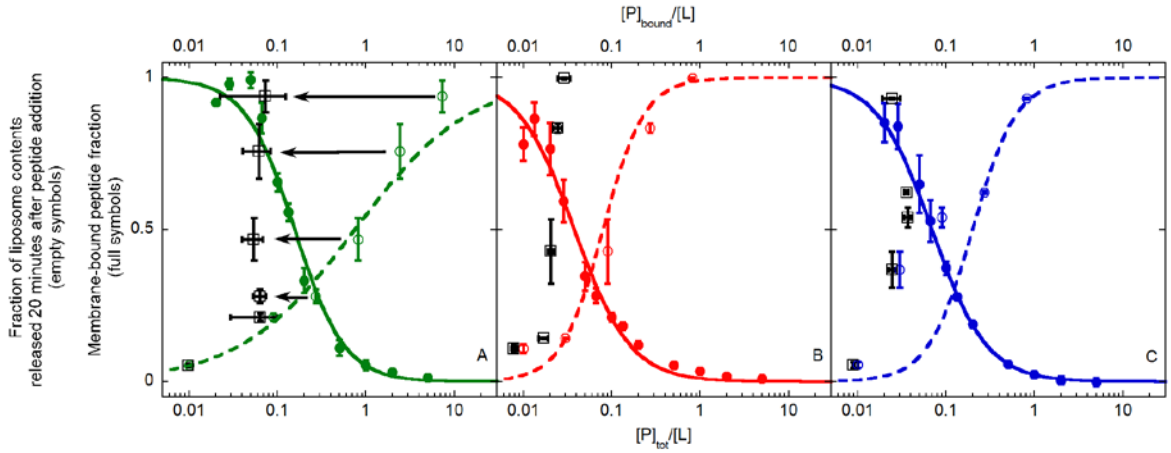

Figure S4. Comparison of peptide binding and membrane leakage experiments.

(A) P9-4; (B) Sub3; (C) Novicidin. Full circles: Membrane-bound peptide fraction as a function of the $\frac{[P]_{tot}}{[L]}$ ratio (lower x-axis). Empty circles: Fraction of liposome contents released 20 min after peptide addition, as a function of the $\frac{[P]_{tot}}{[L]}$ ratio (lower x-axis). Full black circles: Fraction of liposome contents released 20 min after peptide addition, as a function of the $\frac{[P]_{bound}}{[L]}$ ratio (upper x-axis).

The arrows in the first graph represent the shift of released fraction when plotted *vs* $\frac{[P]_{tot}}{[L]}$ or *vs* $\frac{[P]_{bound}}{[L]}$.